



HAL
open science

The evolution of viscoelastic properties of silicone rubber during cross-linking investigated by thickness-shear mode quartz resonator

Amaury Dalla Monta, Florence Razan, Jean-Benoit Le Cam, Grégory Chagnon

► To cite this version:

Amaury Dalla Monta, Florence Razan, Jean-Benoit Le Cam, Grégory Chagnon. The evolution of viscoelastic properties of silicone rubber during cross-linking investigated by thickness-shear mode quartz resonator. 10th European Conference on Constitutive Models for Rubbers (ECCMR), Aug 2017, Munich, Germany. 10.1201/9781315223278-63 . hal-01807447

HAL Id: hal-01807447

<https://hal.science/hal-01807447>

Submitted on 4 Jun 2018

HAL is a multi-disciplinary open access archive for the deposit and dissemination of scientific research documents, whether they are published or not. The documents may come from teaching and research institutions in France or abroad, or from public or private research centers.

L'archive ouverte pluridisciplinaire **HAL**, est destinée au dépôt et à la diffusion de documents scientifiques de niveau recherche, publiés ou non, émanant des établissements d'enseignement et de recherche français ou étrangers, des laboratoires publics ou privés.

The evolution of viscoelastic properties of silicone rubber during cross-linking investigated by thickness-shear mode quartz resonator

A. Dalla Monta^{1,2}, F. Razan², J.-B. Le Cam^{1,3}, G. Chagnon^{4a,4b}

¹University of Rennes 1, Institute of Physics, UMR 6251 - CNRS/Université de Rennes 1, Campus de Beaulieu, 35042 Rennes, France.

²ENS Rennes, SATIE - CNRS 8029, Campus de Ker Lann, 35170 Bruz, France.

³LC-DRIME, Joint Research Laboratory in Imaging, Mechanics and Elastomers, University of Rennes 1/Cooper Standard/CNRS, Campus de Beaulieu, Bât. 10B, 35042 Rennes Cedex, France.

^{4a}Université Grenoble Alpes, TIMC-IMAG, F-38000 Grenoble, France

^{4b}CNRS, TIMC-IMAG, F-38000 Grenoble, France

ABSTRACT: Characterizing the effects of cross-linking level and kinetics on the mechanical properties of rubber, especially viscoelasticity, provides information of importance to better understand and predict its final mechanical properties. Classically, the effects of cross-linking on the mechanical properties are investigated with a rheometer. Typical results give the evolution of elastic properties of rubber in the solid state with respect to time or to the cross-linking level. The frequency of the mechanical loading applied is generally a few Hertz. In the case where the rubber is initially in the liquid state, such as some silicone rubbers, this type of characterization is not suitable anymore. In this study, a new characterization technique based on the Quartz Crystal Microbalance (QCM) principle has been developed in order to characterize the viscoelastic properties (elastic and viscous moduli) of a silicone rubber during cross-linking, *i.e.* from the liquid (uncross-linked) to the solid (final cross-linked) state. The device consists in a Thickness-Shear Mode (TSM) resonator generating ultrasonic waves, which provides viscoelastic properties of a material in contact with its surface from an electrical impedance analysis. In contrast to other characterization tools, it makes possible the continuous and non-destructive characterization of viscoelastic properties from a small material volume, under 1mL. Moreover, frequencies at which these properties are characterized are of the order of magnitude of the megahertz, which provides very complementary results to classical characterization, rather in the order of the hertz.

1 INTRODUCTION

The Quartz Crystal Microbalance (QCM) is a versatile tool, first described in the founder paper work of (Sauerbrey 1959). Because it is a rather simple sensor, it has since then been widely used in sensing applications in various domains, allowing us to determine with precision measurands such as mass density (Stockbridge 1966b), viscosity (Kanazawa and Gordon 1985) and pressure (Stockbridge 1966a), in a continuous and non-destructive manner, with sample as small as a microliter. In mechanics, for instance, it is used for measuring complex shear modulus \tilde{G} in order to characterize a polymer (Holt, Gouws, and Zhen 2006) or follow its evolution during a specific process, such as dissolution (Hinsberg, Willson, and Kanazawa 1986). In biology, where its use continues to increase (Becker and Cooper 2011), the functionalization of the QCM surface with a definite substance allows to measure active species absorption or deposition, and then to recognize specific pathologies like schistosomiasis (Wang et al. 2006) or Ebola fever

(Yu et al. 2006). In chemistry, with a similar method, the sensor can detect presence of harmful molecules in the air, acting as an electronic nose (Si et al. 2007).

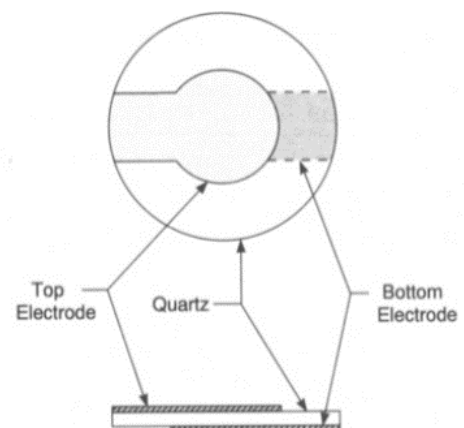


Figure 1. Top and side views of a quartz crystal microbalance (Martin et al. 1993).

The QCM, as shown in figure 1, consists in a circular thin disk of piezoelectric AT-cut quartz, with metallic electrodes on both sides. The application of a voltage between them generates a shear deformation of the

crystal, which can then be excited into resonance when its thickness is near an odd multiple of half the acoustic wavelength. The deposit of a material sample on the crystal changes the resonance properties, and it appears that they are fundamentally dependent on the characteristics, either mechanical or electrical, of the sample.

For all these applications, the QCM needs an electrical interface able to apply a sinusoidal voltage between its electrodes and to measure the resonance conditions. Among all the methods of read-out, the most used is the impedance analysis (Arnau 2008), which maps the electrical admittance of the QCM as a function of the frequency, giving access to a greater number of parameters than simpler methods such as the use of an oscillator circuitry. However, it requires an impedance analyzer, which is typically relatively expensive and hardly mobile. A portable and low-cost solution would therefore be particularly useful, especially in biology, where in situ assays would help patients at home and doctors on the spot, ensure the safety in the entire chain of the food industry or improve the security against biological agents (Nayak et al. 2009). A cheap, simple and robust device is also critical for the commercialization of the whole system, opening the door to the democratization of the associated analysis.

The present paper aims at validating the use of a compact and comparatively cheap network analyzer, the “miniVNA PRO”, as a read-out instrument for the QCM for the characterization of the cross-linking of rubbers. It is organized as follows. Section 2 describes briefly the theory governing the behavior of the QCM and the measurement principle. Section 3 presents the experimental dispositive and the protocol established in order to reduce the influence of external factors. Finally, section 4 analyses the results in light of the aforementioned objectives.

2 THEORETICAL FRAMEWORK

On a fundamental point of view, the QCM is simply a transducer, linking its load impedance with its electrical impedance. The fundamental relations governing its behavior are briefly recalled hereafter. The reader can refer to (Johannsmann 2015) for further information.

2.1 Acoustic parameterization

In a first approximation, when its diameter is large compared to its thickness, the QCM can essentially be seen as a unidimensional device, a succession of homogeneous layers in which acoustic shear waves

propagate along the z axis. Inside a layer, the amplitude $u(t, z)$ of the displacement due to the wave is described by the well-known wave equation, which writes:

$$\frac{\partial^2 u}{\partial t^2} = c^2 \frac{\partial^2 u}{\partial z^2} \quad (1)$$

This can be expressed in the frequency domain by:

$$-\omega^2 \hat{u} = \tilde{c}^2 \frac{d^2 \hat{u}}{dz^2} \quad (2)$$

Here, ω is the angular frequency, $\hat{u}(z)$ is the complex amplitude of the displacement, $\tilde{c} = \sqrt{\rho/\tilde{G}}$ is the speed of sound, ρ the density and \tilde{G} the shear modulus. Introducing the wavenumber $\tilde{k} = \sqrt{\omega/\tilde{c}}$, solutions of the wave equation write in the form of:

$$\hat{u}(z) = \hat{u}^+ \exp(+i\tilde{k}z) + \hat{u}^- \exp(-i\tilde{k}z) \quad (3)$$

\hat{u}^+ and \hat{u}^- are the amplitude of a wave traveling respectively to the left and to the right. It is therefore possible to express the velocity $\hat{v}(z)$ and the shear stress $\hat{\sigma}(z)$:

$$\begin{aligned} \hat{v}(z) &= i\omega \hat{u}(z) \\ &= i\omega \hat{u}^+ \exp(+i\tilde{k}z) + i\omega \hat{u}^- \exp(-i\tilde{k}z) \end{aligned} \quad (4)$$

$$\begin{aligned} \hat{\sigma}(z) &= \tilde{G} \frac{d\hat{u}}{dz} \\ &= i\tilde{k}\tilde{G}\hat{u}^+ \exp(+i\tilde{k}z) - i\tilde{k}\tilde{G}\hat{u}^- \exp(-i\tilde{k}z) \\ &= i\omega\tilde{Z}\hat{u}^+ \exp(+i\tilde{k}z) - i\omega\tilde{Z}\hat{u}^- \exp(-i\tilde{k}z) \end{aligned} \quad (5)$$

2.2 Mason circuit

The acoustic shear wave is very similar to an electromagnetic wave in its behavior (Mason 1941). Establishing an analogy between electrical circuits and mechanical systems, it is therefore possible to represent a layer of the QCM as a distributed-element network. Such a representation is perfectly suitable to this device, because our goal is to link a mechanical quantity with an electrical one.

To go further, since only the quantities at the interfaces between two layers are of interest, the QCM can even be represented as a two-port network, one for each interface. This paragraph shows that the Mason circuit is a compatible representation.

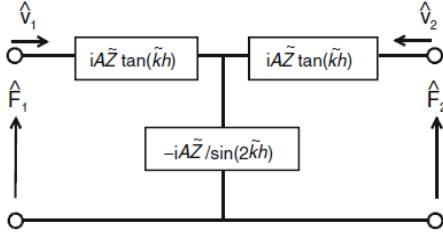


Figure 2. Two-port network representation of a layer in which propagate a shear-wave (Johannsmann 2015).

In figure 2, A is the area of the device in the plane orthogonal to the direction of propagation, and h is half the thickness of the considered layer. Using the Kirchhoff rules, it appears that forces \hat{F} and velocities \hat{v} are linked by the following expressions that should be validated:

$$\hat{F}_1 = iA\tilde{Z} \tan(\tilde{k}h) \hat{v}_1 - \frac{iA\tilde{Z}}{\sin(2\tilde{k}h)} \cdot (\hat{v}_1 + \hat{v}_2) \quad (6)$$

$$\hat{F}_2 = \frac{iA\tilde{Z}}{\sin(2\tilde{k}h)} \cdot \hat{v}_1 - iA\tilde{Z} \tan(\tilde{k}h) \cdot (\hat{v}_1 + \hat{v}_2) \quad (7)$$

The displacement and the shear stress can be written as:

$$\hat{u}(z) = \hat{u}_\alpha \sin(\tilde{k}z) + \hat{u}_\beta \cos(\tilde{k}z) \quad (8)$$

$$\hat{\sigma}(z) = \omega\tilde{Z}(\hat{u}_\alpha \cos(\tilde{k}z) - \hat{u}_\beta \sin(\tilde{k}z)) \quad (9)$$

Hence, being careful about the sign of the relations:

$$\begin{aligned} \hat{F}_1 &= -A\hat{\sigma}(-h) & \hat{v}_1 &= +i\omega\hat{u}(-h) \\ \hat{F}_2 &= -A\hat{\sigma}(h) & \hat{v}_2 &= -i\omega\hat{u}(h) \end{aligned} \quad (10)$$

This yields to the set of equations 6-7 after some mathematical manipulations, confirming the correctness of the circuit used. However, as such, the circuit is still incomplete: the quartz being piezoelectric, a third port electrical in nature should be added, as shown in figure 3. Across a transformer, an electrical source connected to this port will be able to generate an acoustic wave and to be influenced by the mechanical properties of the device, with a conversion factor $\phi = A \cdot e_{26}/(2h)$, where e_{26} is the relevant component of the piezoelectric coupling tensor.

It can be shown that this three-port network satisfies the constitutive relations of piezoelectricity, namely:

$$\hat{\sigma} = \tilde{G} \frac{d\hat{u}}{dz} - \frac{e_{26}}{\tilde{\epsilon}\epsilon_0} \hat{D} \quad (11)$$

$$\hat{E} = -\frac{\tilde{e}_{26}}{\tilde{\epsilon}\epsilon_0} \frac{d\hat{u}}{dz} + \frac{1}{\tilde{\epsilon}\epsilon_0} \hat{D} \quad (12)$$

Finally, in practice and on one side, the QCM is in contact with the air, which has acoustic wave impedance negligible compared with the one of the quartz. Therefore $\hat{F}_1 = 0$, and the equivalent circuit is short-circuited on the left. On the other side, the QCM is in contact with the material to characterize, with acoustic impedance at the interface \tilde{Z}_L . Therefore $\hat{F}_2/\hat{v}_2 = A\tilde{Z}_L$, and the equivalent circuit is closed with a resistance having this value. It remains in the circuit only the electrical port, as illustrated in figure 3, which corresponds to the fact that the QCM can only be interrogated electrically through its electrodes, and not by any acoustic or mechanical ways.

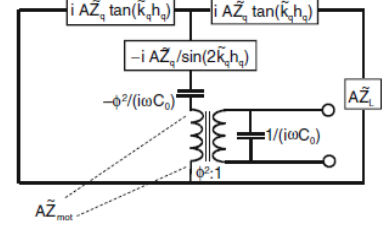


Figure 3. One-port network representation of a quartz crystal microbalance in contact with the air on one side and a specific sample on the other (Johannsmann 2015).

2.3 Resonance condition

Let us now use the Mason circuit to calculate the equivalent impedance of the circuit coming after the transformer, the motional impedance \tilde{Z}_{mot} . Using the Kirchhoff rules, it follows:

$$\begin{aligned} \tilde{Z}_{mot} &= -\frac{\phi^2}{i\omega C_0} - \frac{i\tilde{Z}_q}{\sin(2\tilde{k}_q h_q)} \\ &+ \left((i\tilde{Z}_q \tan(\tilde{k}_q h_q))^{-1} + (i\tilde{Z}_q \tan(\tilde{k}_q h_q) + \tilde{Z}_L)^{-1} \right)^{-1} \end{aligned} \quad (13)$$

This relation can be simplified by assuming that the wavenumber \tilde{k}_q is close to the ideal open-circuit wavenumber $\tilde{k}_{q,OC} = n\pi/2h_q$, solution of the equation $\tilde{Z}_{mot} = 0$ when the QCM is fully immersed in the air without influence of the piezoelectric effect. Using a Taylor expansion of the previous relation yields:

$$\tilde{Z}_{mot} \approx \frac{1}{4} \left(-\frac{4\phi^2}{i\omega C_0} + in\pi\tilde{Z}_q \frac{\tilde{\omega} - \tilde{\omega}_{OC}}{\tilde{\omega}_{OC}} + \tilde{Z}_L \right) \quad (14)$$

This relation can then be applied twice: first, in the unloaded reference state (the resonant angular frequency being called $\tilde{\omega}_{ref}$) with $\tilde{Z}_L = 0$; secondly, in charge (the resonant angular frequency being called $\tilde{\omega}_{sample}$). Calculating the frequency shift by using the resulting equations brings the so-called Gordon–Kanazawa–Mason result:

$$\frac{\Delta f}{f_0} = \frac{\tilde{\omega}_{ref} - \tilde{\omega}_{sample}}{\frac{\tilde{\omega}_{OC}}{n}} = \frac{i}{\pi \tilde{Z}_L} \quad (15)$$

This is a direct relation between frequencies measurement and the load impedance of the tested sample. To go further, it is assumed that the sample is a semi-infinite medium and equations 4 and 5 yield:

$$\frac{\hat{\sigma}(z)}{\hat{v}(z)} = \frac{i\omega \tilde{Z}_{sample} \hat{u}^+ \exp(+i\tilde{k}_{sample}z)}{i\omega \hat{u}^+ \exp(+i\tilde{k}_{sample}z)} = \tilde{Z}_{sample} \quad (16)$$

Hence:

$$\tilde{Z}_L = \frac{\hat{\sigma}(h_q)}{\hat{v}(h_q)} = \tilde{Z}_{sample} = \sqrt{\rho_{sample} \tilde{G}_{sample}} \quad (17)$$

Given that the density of the sample is already known, the shear modulus can be deduced. Of course, the quantities characterizing the quartz in the previous relation (\tilde{Z}_q and f_0) are not known a priori. However, they can be evaluated by making an additional measurement with a sample in a well-known material, for instance water.

2.4 Extraction of the resonance properties

The impedance analyzer used in these experiments measures the electrical admittance $\tilde{Y}_{el,measure}$ as a function of the frequency. This paragraph explains how the complex resonance frequency can be deduced from this measurement. It can be shown that the linearization around the open-circuit frequency used previously allows getting a simpler representation of the equivalent circuit, using only standard electrical elements (resistance, inductance and conductance). That is the well-known Butterworth-Van-Dyke model, shown in figure 4.

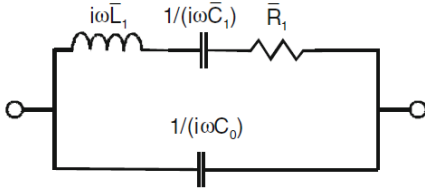


Figure 4. Electrical circuit associated with Butterworth-Van-Dyke model (Johannsmann 2015).

The Kirchhoff rules yield the electrical admittance of this circuit:

$$\tilde{Y}_{el} = i\omega\bar{C}_0 + \left(i\omega\bar{L}_1 + \frac{1}{i\omega\bar{C}_1} + \bar{R}_1 \right)^{-1} \quad (18)$$

It is possible to fit the measurement $\tilde{Y}_{el,measure}(\omega)$ with this theoretical $\tilde{Y}_{el}(\omega)$ and deduce the complex

resonance frequency from the values of the four elements, but it is helpful to use directly the following expanded Lorentzian functions, that reduce the scatter in the fit parameters:

$$\Re(\tilde{Y}_{el}) = G_{el,max} \Gamma \frac{f}{f_r} \left(\frac{\Gamma}{(f_r-f)^2 + \Gamma^2} \cos(\theta) + \frac{f_r-f}{(f_r-f)^2 + \Gamma^2} \sin(\theta) \right) + G_{el,off} \quad (19)$$

$$\Im(\tilde{Y}_{el}) = G_{el,max} \Gamma \frac{f}{f_r} \left(\frac{\Gamma}{(f_r-f)^2 + \Gamma^2} \cos(\theta) - \frac{f_r-f}{(f_r-f)^2 + \Gamma^2} \sin(\theta) \right) + B_{el,off} \quad (20)$$

The complex resonant frequency is then simply deduced from these parameters:

$$\tilde{f}_r = f_r + i\Gamma \quad (21)$$

3 MATERIALS AND METHODS

The quartz crystal and its holder used in the experiments are the commercially available QCM200 (Stanford Research Systems, CA, USA). The crystal has a resonance frequency near 5 Mhz and a diameter of 2.54 cm. It is covered with circular electrodes of titanium and gold. It is physically maintained with one O-ring on both side and connected with the electrical interface via BNC connectors, which are then adapted to an SMA connection. The portable network analyzer is the miniVNA PRO (mini Radio Solutions, Germany), shown in figure 5.



Figure 5. Photograph of the network analyzers used in the experiment: the mini-VNA PRO.

The QCM is placed inside a thermostatic chamber at a given controlled temperature. The network analyzer is initially calibrated by the short-open-load method. The quartz crystal is washed with acetone, rinsed with water and dry with nitrogen before being placed inside its holder. Once the resonance frequency is stabilized, the crystal is loaded with a volume of 900 μL of distilled water as the reference material, creating a layer thick enough to be considered semi-infinite. Finally, after stabilization of the resonance frequency, the water is removed and replaced by the same volume of 900 μL of PDMS rubber RTV615 (Momentive) in the liquid state, *i.e.* non cross-linked. Thus, the evolution of the viscoelastic properties will be measured continuously from the liquid (uncross-linked) state to the solid (cross-linked) state.

4 RESULTS

Figure 6 gives the evolution of the viscoelastic properties in terms of shear modulus G' (a) and loss factor $\tan \delta$ (b) at different ambient temperatures, respectively $25\text{ }^{\circ}\text{C}$, $50\text{ }^{\circ}\text{C}$ and $80\text{ }^{\circ}\text{C}$. At $25\text{ }^{\circ}\text{C}$, the value of the shear modulus is stabilized from 35 hours on. Its evolution is strongly nonlinear from 4 MPa for the liquid state (only slightly cross-linked) to the stabilized value of 12 MPa for the solid state. These values are high compared to values obtained under classical mechanical spectroscopy characterization, which is consistent with the fact that the frequency we applied is in the MHz domain, *i.e.* much higher than classical characterization tests. Moreover, three regimes of evolution of the elastic modulus are observed, as illustrated by the dotted line in figure 6, which can be associated with variation in the cross-linking kinetics. The loss factor decreases in a same nonlinear way from 1.6 to 0.8.

While illustrating a similar behavior, the curves obtained at $50\text{ }^{\circ}\text{C}$ and $80\text{ }^{\circ}\text{C}$ highlight that the higher the temperature, the faster the evolution of viscoelastic properties. Such results are no more discussed in the present paper, which only aims at presenting QCM technology as a new way of investigation of the cross-linking from liquid to solid state and at different temperatures.

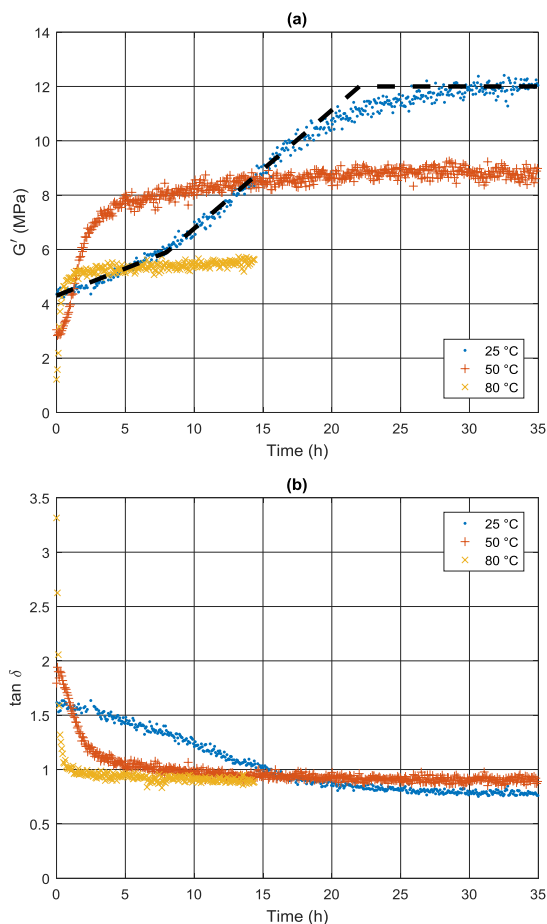


Figure 6. Evolution of the shear modulus (a) and the loss factor (b) of PDMS from the liquid to the solid state.

5 CONCLUSION AND PERSPECTIVES

The paper aims at presenting the QCM as a relevant tool for measuring the viscoelastic properties of rubbers in the MHz domain. The advantage of such a technique is the fact that the measurement can be carried out for liquids as well for solids, *i.e.* for rubbers from the uncross-linked to the cross-linked state, with a small material volume.

The kinetics of cross-linking and the nonlinear relationship between the number of cross-links and the mechanical properties can therefore be quantified and investigated through the variation in the viscoelastic response.

6 REFERENCES

- Arnau, Antonio. 2008. "A Review of Interface Electronic Systems for AT-Cut Quartz Crystal Microbalance Applications in Liquids." *Sensors* 8 (1): 370–411.
- Becker, Bernd, and Matthew A Cooper. 2011. "A Survey of the 2006–2009 Quartz Crystal Microbalance Biosensor Literature." *Journal of Molecular Recognition* 24 (5): 754–787.
- Hinsberg, WD, CG Willson, and KK Kanazawa. 1986. "Measurement of Thin-Film Dissolution Kinetics Using a Quartz Crystal Microbalance." *Journal of The Electrochemical Society* 133 (7): 1448–1451.
- Holt, Robert C., Gideon J. Gouws, and John. Z. Zhen. 2006. "Measurement of Polymer Shear Modulus Using Thickness Shear Acoustic Waves." *Current Applied Physics* 6 (3): 334–39. doi:10.1016/j.cap.2005.11.013.
- Johannsmann, Diethelm. 2015. *The Quartz Crystal Microbalance in Soft Matter Research: Fundamentals and Modeling*. 1st ed. Soft and Biological Matter. Springer International Publishing. <https://books.google.fr/books?id=IkAqBAAAQBAJ>.
- Kanazawa, K. Keiji, and Joseph G. Gordon. 1985. "The Oscillation Frequency of a Quartz Resonator in Contact with Liquid." *Analytica Chimica Acta* 175: 99–105. doi:10.1016/S0003-2670(00)82721-X.
- Martin, Stephen J., Gregory C. Frye, Antonio J. Ricco, and Stephen D. Senturia. 1993. "Effect of Surface Roughness on the Response of Thickness-Shear Mode Resonators in Liquids." *Analytical Chemistry* 65 (20): 2910–2922. doi:10.1021/ac00068a033.
- Mason, WP. 1941. "Electrical and Mechanical Analogies." *Bell System Technical Journal* 20 (4): 405–414.
- Nayak, Madhura, Akhil Kotian, Sandhya Marathe, and Dipshikha Chakravorty. 2009. "Detection of Microorganisms Using Biosensors — A Smarter Way towards Detection Techniques." *Biosensors and Bioelectronics* 25 (4): 661–667.
- Sauerbrey, Günter. 1959. "Verwendung von Schwingquarzen zur Wägung dünner Schichten und zur

Mikrowägung." *Zeitschrift für Physik* 155 (2): 206–222.

- Si, Pengchao, John Mortensen, Alexei Komolov, Jens Denborg, and Preben Juul Møller. 2007. "Polymer Coated Quartz Crystal Microbalance Sensors for Detection of Volatile Organic Compounds in Gas Mixtures." *Analytica Chimica Acta* 597 (2): 223–230.
- Stockbridge, CD. 1966a. "Effects of Gas Pressure on Quartz Crystal Microbalances." *Vacuum Microbalance Techniques* 5: 147–178.
- . 1966b. "Resonance Frequency versus Mass Added to Quartz Crystals." *Vacuum Microbalance Techniques* 5: 193.
- Wang, Hua, Yun Zhang, Bani Yan, Li Liu, Shiping Wang, Guoli Shen, and Ruqin Yu. 2006. "Rapid, Simple, and Sensitive Immunoagglutination Assay with SiO₂ Particles and Quartz Crystal Microbalance for Quantifying *Schistosoma Japonicum* Antibodies." *Clinical Chemistry* 52 (11): 2065–2071.
- Yu, Jae-Sung, Hua-Xin Liao, Aren E Gerdon, Brian Huffman, Richard M Searce, Mille McAdams, S Munir Alam, et al. 2006. "Detection of Ebola Virus Envelope Using Monoclonal and Polyclonal Antibodies in ELISA, Surface Plasmon Resonance and a Quartz Crystal Microbalance Immunosensor." *Journal of Virological Methods* 137 (2): 219–228.